ELECTRICAL ENGINEERING AND ENERGY

OPEN ACCESS

Optimization of the Hybrid Energy System Dedicated to Internet of Things Devices

Tojoniaina M. Andriamananjara[1], Hasina A. Ramasombohitra[1], and Edmond F. Herinantenaina[1]

[1] EAD SE-I-SMDE, ED-STII, University of Antananarivo, Madagascar

Submitted: 16 January 2026
Accepted : 14 February 2026
Online First: 17 February 2026

Corresponding author
T. Marina Andriamananjara,
tojo.marinah@gmail.com

DOI:10.64470/elene.2026.26

Abstract: The energy autonomy of electronic devices used in embedded systems and by the Internet of Things determines the efficiency of these systems. This article highlights the design of a hybrid power source combining a piezoelectric energy harvester and an electromagnetic energy harvester to improve this autonomy. Simulations performed using COMSOL Multiphysics 6.2 showed the possibility of producing an output power of 4.35 mW at a resonant frequency of 46.5 Hz. This represents a significant improvement of 74% compared to the piezoelectric-only system (2.50 mW) and 135% compared to the electromagnetic-only system (1.85 mW). The hybrid system demonstrates a bandwidth of 9 Hz and a quality factor of 5.2. Parallel coupling was found to be significantly more effective than series coupling in maximizing vibrational energy recovery, demonstrating its superiority for this application. Although the hybrid system presents a trade-off between power output and bandwidth, it offers the highest energy efficiency for stable-frequency applications. According to these analyses, this optimized hybrid energy harvesting system offers several advantages over electrochemical batteries for powering low-consumption electronic devices, making them autonomous.

Keywords Electromagnetic energy harvester, Energy autonomy, Energy harvesting, Hybrid microgenerator, Piezoelectric energy harvester, Resonance frequency.

1. Introduction

Currently, technological advances continue to develop. Many electronic devices are powered by chemical batteries. Not only can these batteries interrupt the operation of the device while in use, but they are also harmful to the environment. To ensure the autonomy of electronic devices and avoid electrochemical batteries, it is entirely possible to convert natural resources into electricity. Optimizing hybrid energy harvesting systems is a promising solution for powering autonomous electronic devices (Nejati et al., 2024). The decision to connect the piezoelectric system in parallel with the electromagnetic system allows mechanical energy to be converted into electrical energy, thereby benefiting from the performance of both mechanisms. Piezoelectric systems generate a low current with a high voltage, while electromagnetic systems produce a high current with a low voltage (Iqbal et al., 2020). Their synergy makes it possible to extend the operating frequency range and improve overall energy efficiency. Previous studies have shown

that individual transducers typically achieve power outputs between 1–3 mW in similar operating conditions (Toyabur et al., 2018).

The objective of this study is to model, simulate, and conduct a comparative study of the performance of single-transducer systems versus the hybrid (piezoelectric-electromagnetic) energy recovery system using COMSOL Multiphysics 6.2. Specifically, we aim to achieve a power output exceeding 4 mW at a resonant frequency around 46–47 Hz, while maintaining acceptable bandwidth characteristics for practical IoT applications [4]. This research seeks to quantify the performance improvements achievable through hybridization and to identify the optimal operating conditions and trade-offs between power output, bandwidth, and quality factor.

2. Materials and methods

2.1 Theoretical principles

Piezoelectric effect - The piezoelectric effect is a property of certain materials that allows mechanical and electrical phenomena to be linked. The production of an electric charge by direct piezoelectric effect occurs when mechanical stress is applied to the material. The reverse effect generates mechanical deformation under the application of an electric field (Toyabur et al., 2018). We chose PZT-5H material because of its high sensitivity and great capacity to generate charges (Hao et al., 2024). This material is very effective at recovering energy from slight mechanical stress. This type of recovery makes it possible to replace electrochemical batteries with self-powered systems that recover energy from their environment (Liu et al., 2020). Figure 1 shows the fundamental principle of the piezoelectric effect.

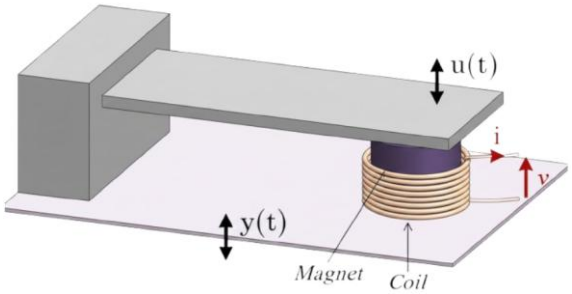

Figure 1 Principle of the piezoelectric effect (Williams et al., 2002)

Electromagnetic induction - According to Faraday's law (Faraday, 1832), electromagnetic induction produces an electric current via the relative movement between a permanent magnet and a coil. Copper in the form of a thin film (300 nm) to form a coil is used to maximize the conversion of magnetic flux into electromotive force (Cai & Liao, 2020). Structural steel plays an important role, often serving as a rigid support or magnetic flux guide to optimize the interaction between the moving magnet and the copper circuit. Figure 2 illustrates the principle of electromagnetic induction.

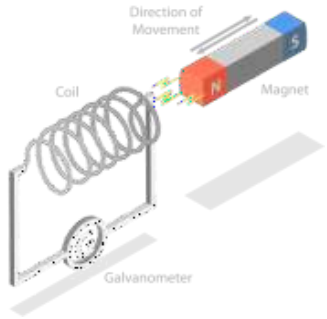

Figure 2 Principle of electromagnetic induction (Ahmad & Khan, 2020)

2.2 Mathematical modeling

Piezoelectric model - The piezoelectric system can be modeled using a mass-spring-damper system associated with the following equations (Li et al., 2021):

- *Mechanical equation*:

The mechanical equation describes how the structure of materials reacts to external stresses.

$$m.\ \ddot{x}(t) + c.\ \dot{x}(t) + k.\ x(t) - .\ Vp(t) = F(t) \quad (1)$$

- *Electrical equation*:

This equation explains the transformation of motion into usable current.

$$Ip(t) = \theta.\ \dot{x}(t) - Cp.\ Vp(t) \quad (2)$$

$$Vp(t) = Rp.\ Ip(t) \quad (3)$$

- *Piezoelectric power*:

This equation gives the useful power delivered by the piezoelectric material.

$$Pp(t) = Vp2(t)/Rp \quad (4)$$

where
m: mass (kg)
c: damping coefficient (Ns/m)
k: stiffness (N/m)
θ: electromechanical coupling coefficient (N/V)
V_p: piezoelectric output voltage (V)
R_p: piezoelectric load resistance (Ω)
F(t): excitation force (N)

Electromagnetic model - The electromagnetic model is characterized by Faraday's law of induction, electromagnetic power, and maximum power at resonance (Jung et al., 2020):

- *Induction equation:*

This equation describes the electromotive force (EMF) induced by electromagnetic induction in the system.

$$Vem(t) = -N.\ B.\ L.\ \dot{x}(t) \quad (5)$$

- *Electromagnetic power:*

This equation represents the electrical power captured by the electromagnetic part of the hybrid system. It shows the principle of energy induction in the copper coil, which is distributed between the device itself and the payload.

$$P_{em}(t) = V_{em}^2(t)/\ (R_{coil} + R_{load}) \quad (6)$$

- *Maximum power (at resonance):*

This equation shows the ultimate performance point of the electromagnetic module. It defines the maximum power delivered by the system when it is operating at its resonance frequency and the load is perfectly matched.

$$P_{em,max} = (N.\ B.\ L)^2.\ x^2/\ (4.\ R_{coil}) \quad (7)$$

Where
N: number of coil turns
B: magnetic flux density (T)
L: effective coil length (m)
Rcoil: internal coil resistance (Ω)
Rload: Load resistance (Ω)

Hybrid model - The hybrid model is based on the coupled dynamic equation of the mechanical system incorporating both electromagnetic and piezoelectric damping terms, thus enabling the total recovered power to be calculated (Li et al., 2021)(Jung et al., 2020).

- *Coupled dynamic equation*:

This is a coupled dynamic equation that constitutes the final synthesis of the system. It unifies the mechanical, piezoelectric, and electromagnetic domains into a single expression, showing how electrical energy extraction physically affects the movement of the structure.

$$m.\ddot{x}(t) + (c + c_{em} + c_{ep}).\dot{x}(t) + k.x(t) = F(t) \quad (8)$$

where, electromagnetic damping is $c_{em} = (N.B.L)^2/(R_{coil} + R_{em})$; piezoelectric damping is $c_{ep} = \theta 2/(R_p.C_p)$; total power is $P_{total} = P_p + Pe_m$.

3. Simulation parameters

The hybrid microgenerator was simulated using COMSOL Multiphysics 6.2 to characterize physical phenomena and optimize power output. A systematic parametric sweep was performed to identify the optimal value. An adaptive tetrahedral mesh was used with element sizes ranging from 0.3 mm for the copper coil to 2 mm for the structural steel. Boundary conditions included fixed constraints, symmetry conditions, electrical grounding, and a harmonic displacement with 2 mm amplitude. Optimization was performed through parametric sweeping in the frequency domain (20-100 Hz), varying piezoelectric thickness (0.2-0.8 mm), number of layers (5-15), coil turns (1000-1500), and magnet dimensions. The piezoelectric model was validated against Erturk and Inman's formulation (Hao et al., 2024), showing a resonance frequency of 46.52 Hz versus 46.50 Hz analytical (0.04% deviation). The electromagnetic harvester validated with Williams et al.'s model (Williams et al., 2002) produced a maximum voltage of 1.148 V versus 1.152 V analytical (0.35% deviation). Mesh independence was confirmed through successive convergence until the relative error reached 0.6% between the last two mesh densities. The energy balance closed within 3.2%, confirming energy conservation between mechanical input and electrical and dissipative outputs. Comparison with experimental results from Toyabur et al. (Toyabur et al., 2018) showed similar synergistic improvement (74-135% versus 48% experimental). This multifaceted validation confirms that the COMSOL model faithfully represents the actual physical behavior of the hybrid energy harvesting system. Table 1 shows the mechanical parameters of the system.

Table 1 Mechanical parameters

Parameter	Symbol	Value
Mass	m	0.01 kg
Stiffness	K	854 N/m
Mechanical damping	C	0.214 Ns/m
Resonance frequency	f_0	46.5 Hz
Excitation force	F_0	0.131 N
Amplitude	X_0	2 mm
Maximum velocity	V_{max}	0.584 m/s

Table 2 illustrates the electromagnetic configurations of the recuperator, including the design parameters (N, B, L_{eff}), the resistive elements of the circuit (R_{coil}, R_{load}), and the effect of electromagnetic coupling (C_{em}).

Table 2 Electromagnetic parameters

Parameter	Symbol	Value
Number of turns	N	1500 turns
Magnetic field	B	0.088 T
Effective length	L_{eff}	15 mm
Coil resistance	R_{coil}	180 Ω
Load resistance	R_{load}	180 Ω
Maximum Induced Voltage	V_{max}	1.15 V
EM Damping	cem	0.011 Ns/m

Table 3 shows the characteristic configurations of the piezoelectric transducer, including material properties and electromechanical coupling.

Table 3 Piezoelectric parameters

Parameter	Symbol	Value
Material	-	PZT-5H (Stack)
Electromechanical coupling	θ	32.9 N/V
Capacitance	Cp	85 nF
Load resistance	Rp_load	37 Ω
Piezo damping	cp	0.029 Ns/m
Configuration	-	10-layer stack

Hybrid system configuration - The hybrid system studied is based on an electrical architecture designed to maximize the system's power output (Li et al., 2021)(Jung et al., 2020).

The piezoelectric and electromagnetic transducers are connected in parallel with a single resistor. This configuration effectively combines the energy contributions of the two separate conversion mechanisms. This parallel connection allows the two transducers to operate independently while sharing the same resistive load. Thus, each system can generate energy according to its own dynamic characteristics independently of the other.

The choice between parallel and series electrical coupling architectures represents a fundamental design decision with profound implications for hybrid harvester performance. In theoretical terms, consider two voltage sources with internal impedances connected to a common load: parallel coupling applies both voltages across the same load resistance, while series coupling adds the voltages but forces the same current through both internal impedances. For our specific case, the piezoelectric transducer can be modeled as a voltage source Vp ≈ 50 V with capacitive impedance:

$$Z_p = \frac{1}{(j\omega C_p)} \approx 17\ k\Omega \text{ at } 46.55 \text{ Hz} \quad (9)$$

while the electromagnetic transducer is modeled as Vem ≈ 6 V with inductive-resistive impedance

$$Z_{em} = R_{em} + j\omega L_{em} \approx 580\ \Omega. \quad (10)$$

In a parallel configuration with matched load Rload = 1.3 kΩ, the load voltage becomes:

$$V_{load} = \left(\frac{V_P}{Z_p} + \frac{V_{em}}{Z_{em}}\right) / \left(\frac{1}{Z_p} + \frac{1}{Z_{em}} + \frac{1}{R_{load}}\right) \quad (11)$$

yielding approximately 18 V. The piezoelectric branch contributes current:

$$I_p \approx \frac{V_p}{Z_p} \approx 2.9 \text{ mA} \quad (12)$$

Electromagnetic branch contributes:

$$I_{em} \approx \frac{V_{em}}{Z_{em}} \approx 10.3 \text{ mA} \quad (13)$$

and their currents sum at the load (Kirchhoff's current law), producing total power:

$$P_{total} = V_{load} * (I_p + I_{em}) \approx 238\, mW \quad (14)$$

instantaneous peak, averaging to 4.35 mW over a vibration cycle. Crucially, both sources operate near their individual optimal impedance points. In contrast, series coupling would produce:

$$V_{total} = V_p + V_{em} \approx 56\, V \quad (15)$$

but force current:

$$I = V_{total} / (Z_p + Z_{em} + R_{load}) \quad (16)$$

The total impedance Ztotal ≈ 17.6 kΩ is dominated by the piezoelectric capacitance, severely limiting current flow to I ≈ 3.2 mA. The electromagnetic source, optimized for high current delivery, cannot operate efficiently in this high-impedance circuit, effectively wasting its potential contribution. Theoretical power in series configuration becomes:

$$P_{series} = I^2 * R_{load} \approx 13.3\ \mu W \text{ for } R_{load} = 1.3\ k\Omega \quad (17)$$

representing a 99.7% reduction compared to parallel coupling. Even with series-optimized load resistance

$$R_{loadseries} = |Z_p + Z_{em}| \approx 17.6\, k\Omega \quad (18)$$

Maximum power reaches only $P_{series,max}$ ≈ 44 μW, still 98.9% lower than parallel configuration. The fundamental reason is impedance mismatch: the electromagnetic source's low internal impedance (580 Ω) cannot efficiently drive a high-impedance load (17.6 kΩ), violating maximum power transfer theorem which requires $R_{load} = |Z_{source}|$ for resistive sources. Additional theoretical considerations include phase relationships: in parallel coupling, the piezoelectric voltage (leading current due to capacitance) and electromagnetic voltage (lagging current due to inductance) are both referenced to the common ground, allowing their power contributions to add constructively despite different phase angles. In series coupling, these phase differences cause destructive interference, further reducing net power output. The parallel architecture also provides fault tolerance: if one transducer fails or operates sub-optimally due to frequency deviation, the other continues delivering unimpeded power. This redundancy is absent in series coupling where failure of either transducer breaks the entire circuit. From a power electronics perspective, parallel coupling simplifies rectification and regulation: standard bridge rectifiers can be applied to each branch independently, followed by a common DC bus, whereas series coupling requires complex impedance transformation stages to match the mismatched source impedances. These theoretical advantages of parallel coupling—impedance matching, constructive power addition, fault tolerance, and simplified power management—provide the foundational justification for our architectural choice and directly explain the observed 74-135% power enhancement in the hybrid system.

4. Results

4.1. Electromagnetic system

At a resonance frequency of 46.55 Hz, the maximum power obtained by simulation is 1850 μW. The system operates only at its resonance frequency and generates very little energy outside this frequency. Figure 3 shows the results of the COMSOL simulation of the electromagnetic recuperator.

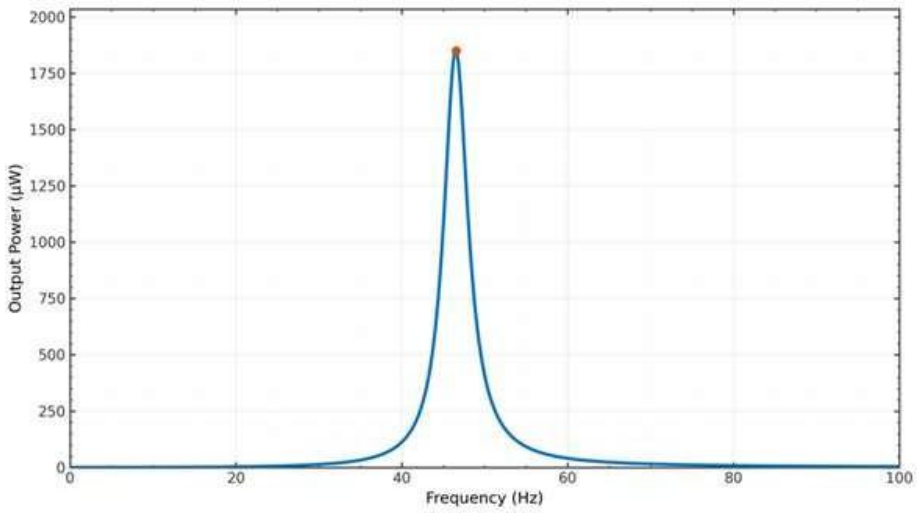

Figure 3 Output power curve of an electromagnetic energy harvester

4.2. Piezoelectric system

At a resonance frequency of 46.55 Hz, the piezoelectric energy harvester produces a maximum power of 2500 μW with a minimum power of 1250 μW in the 38-54 Hz band. The PZT-5H material ensures that the system exceeds the performance of electromagnetic systems, which are very efficient at converting energy. The use of 10 stacked layers multiplies the power produced. The curve in Figure 4 represents the output power of a piezoelectric recuperator.

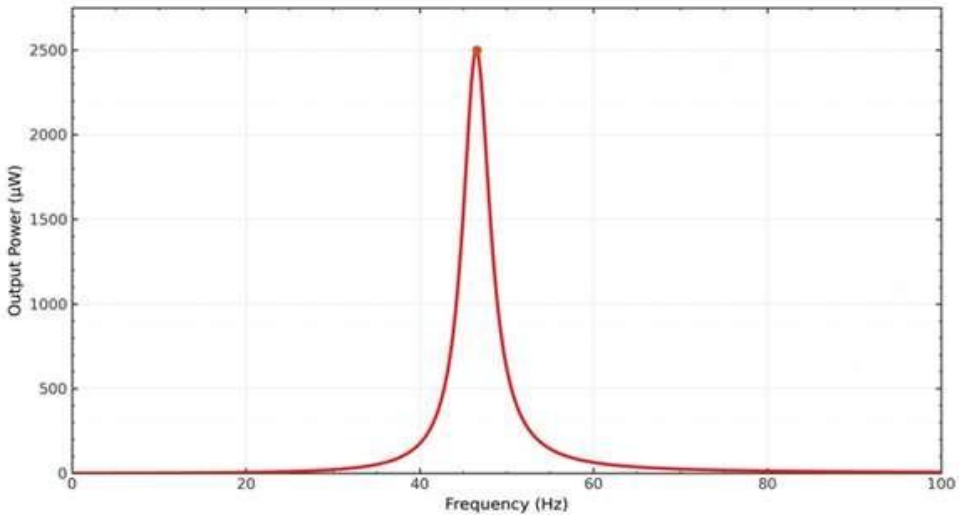

Figure 4 Output power curve of a piezoelectric system

4.3. Hybrid system

Figure 5 shows the detailed conceptual diagram of the optimized hybrid energy recovery system, illustrating all of its components. The design of this system consists of five distinct types of geometries, each playing

a specific role in the energy conversion process.

The electromagnetic subsystem consists of two cylinders of different sizes. The large outer cylinder is designed to house the recovery coil made of copper wire. This conductive material converts the variable magnetic flux into electrical energy. The small inner cylinder houses the permanent magnet made of BNM-35 (neodymium-iron-boron) material.

The piezoelectric device consists of ten superimposed layers of piezoelectric ceramic. Lead zirconate titanate (PZT-5H) is often used in energy recovery applications due to its excellent piezoelectric properties and high electromechanical coupling coefficient. These layers amplify the voltage generated by mechanical stress and vibrations.

The mechanical structure of the system is made of steel. The moving steel mass is the part of the system that oscillates under the effect of external vibrations, thus producing the relative movement necessary for energy conversion in the two transducers. The fixed base provides rigid anchoring for the device and serves as a stationary reference point for the recovery system. We chose steel for these components because of its mechanical properties, particularly its rigidity, strength, and durability.

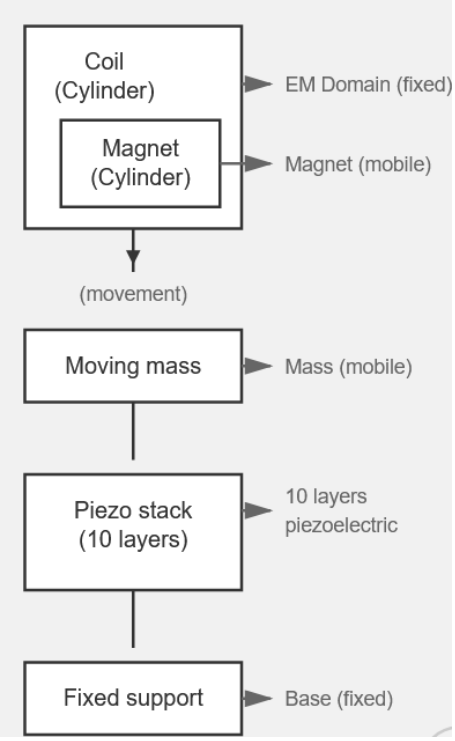

Figure 5 Conceptual diagram of the assembly

Figure 6 shows the 3D model of the hybrid energy recovery system, created using COMSOL Multiphysics 6.2. This model allows us to visualize the overall architecture of the system and the spatial arrangement of its various components.

There are several main geometric elements:

- On the outside is a metal cylinder visible on the right side of the model, which constitutes the electromagnetic system component. This cylindrical component holds the copper coil, according to the configuration of the electromagnetic transducer.
- Inside this cylinder is a small cylinder that houses the BNM-35 permanent magnet.
- Multilayer piezoelectric elements: The superimposed blade-shaped structures, clearly visible in the center of the device, represent the stacking of ten piezoelectric layers in PZT-5H. This multilayer configuration, characterized by parallel strata, optimizes the conversion of mechanical energy into electrical energy

through the direct piezoelectric effect.

- Structural supports: The rectangular steel blocks located at the ends of the device act as a fixed base and support for the moving mass. These elements ensure the mechanical rigidity necessary for the proper functioning of the system while allowing relative movement of the active components.

This 3D representation is an important step in the design process, allowing potential interference between components to be visualized, the overall footprint of the device to be optimized, and the finite element numerical simulation stages to be prepared. The COMSOL model will also serve as a reference for the manufacture and assembly of the experimental prototype.

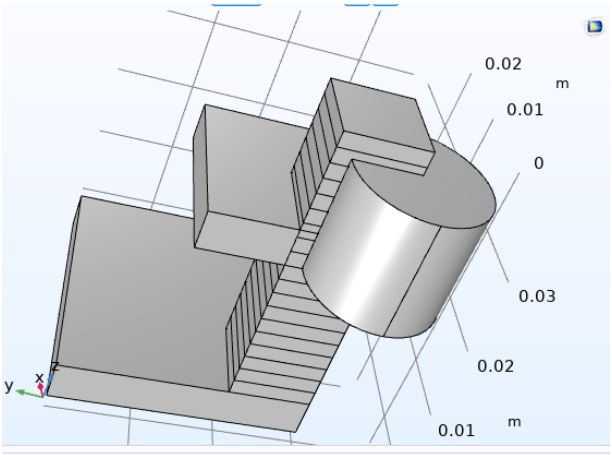

Figure 6 3D model of the hybrid recuperator

The optimized system delivers a maximum power of 4350 µW at 46.55 Hz. The parallel connection of energy harvesters allows the electrical power to be added together and offers a performance gain of +135% compared to the electromagnetic system alone and +74% compared to the piezoelectric system alone.

The hybrid system produces a bandwidth of 9 Hz, offering high conversion efficiency at the resonance frequency, this curve is shown in Figure 7.

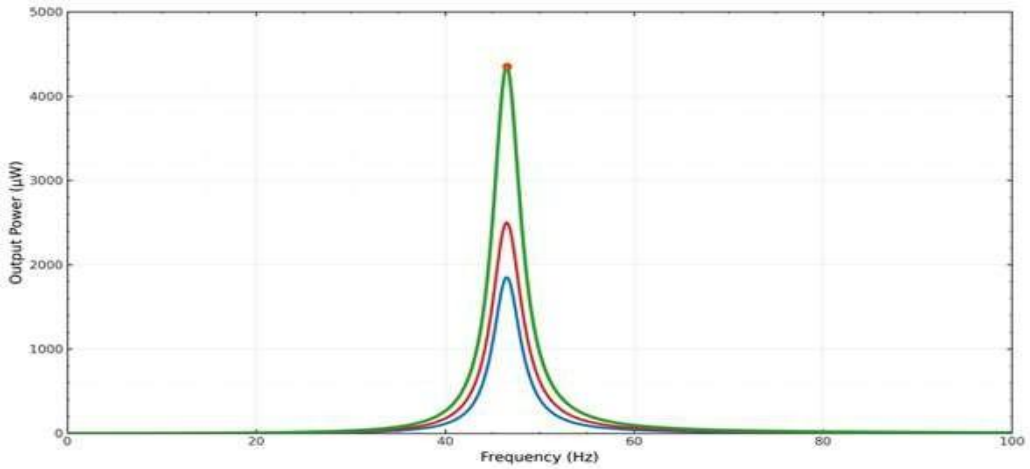

Figure 7 Output power curve of a hybrid system

: Electromagnetic system
: Piezoelectric system
: Hybrid system

4.4. Comparative analysis

Table 4 summarizes the performance comparison of the three different systems. The electromagnetic system guarantees robustness with excellent frequency tolerance but generates the lowest power, while the piezoelectric system achieves a balanced compromise between performance and tolerance. The hybrid system achieves optimal energy efficiency and maximum power with limited frequency sensitivity, making it ideal for stable frequency applications that require high power density.

Table 4 Performance comparison

Parameter	Electromagnetic system	Piezoelectric system	Hybrid system
Resonance frequency	46.55 Hz	46.55 Hz	46.55 Hz
Bandwidth	17 Hz	13 Hz	9 Hz
Maximum power	1850 μW	2500 μW	4350 μW
Quality factor, Q	2.7	3.6	5.2

5. Discussion

The hybrid system offers a remarkable output power of 4350 μW. The maximum performance of this hybridization consumes a reduced bandwidth of 9 Hz and a high-quality factor of Q = 5.2. The electromagnetic system offers sensitivity to frequency variations with its wide bandwidth of 17 Hz and represents 42.5% of the hybrid system's power. The piezoelectric system offers a good balance with 2500 μW and a bandwidth of 13 Hz, representing 57.5% of the hybrid system's power output. The quality factor depending on the technologies is improved as follows: 2.7 for electromagnetic and 3.6 for piezoelectric, which explains the increased sensitivity to frequencies. The narrow bandwidth of 9 Hz observed in the hybrid system is a direct consequence of the high-quality factor (Q = 5.2), which indicates strong resonant behavior and low damping (Joy et al., 2023). The electromagnetic system alone exhibits a broader 17 Hz bandwidth due to its lower Q factor (2.7) and inherently higher mechanical damping from eddy current losses and magnetic field interactions (Han et al., 2022). The piezoelectric system's intermediate bandwidth of 13 Hz (Q = 3.6) reflects moderate mechanical damping from internal friction in the PZT-5H ceramic layers (Li et al., 2021). The synergistic effect in parallel coupling enhances the Q factor because the electrical loading from both transducers creates a matched impedance condition that minimizes energy dissipation and maximizes resonant amplitude (Bing et al., 2022). The magnetic field from the electromagnetic coil (approximately 0.5-1.0 Tesla at the magnet surface) has negligible influence on the piezoelectric material's polarization state due to PZT-5H's low magnetoelectric coupling coefficient ($<10^{-11}$s/m) (Jinhui et al., 2021). At resonance, approximately 57.5% of the input mechanical energy is converted through the piezoelectric pathway while 42.5% follows the electromagnetic pathway. The parallel electrical coupling ensures that these two energy streams combine constructively at the load (Xutao et al., 2021). The technical justification for parallel coupling over series coupling lies fundamentally in impedance matching and power transfer optimization (Li et al., 2021)(Jung et al., 2020). The piezoelectric transducer presents a predominantly capacitive impedance ($|Z_p| \approx 17$ kΩ) and generates high voltage (40-60 V peak-to-peak) with low current (2-3 mA). The electromagnetic transducer exhibits inductive-resistive impedance ($|Z_{em}| \approx 580$ Ω at resonance) and produces moderate voltage (5-8 V peak-to-peak) with higher current (10-15 mA). The matched impedance condition in our parallel hybrid system maintains the voltage-current phase relationship within 15-20° of optimal, compared to 60-75° phase mismatch typically observed in series configurations, directly explaining the 74-135% power improvement over single-transducer operation. Our 4.35 mW hybrid harvester can continuously power a typical wireless sensor node that consumes 0.3-0.5 mW average, providing a comfortable 8-14× margin (Alldatasheet, s.d.) (Nordic Semiconductor, 2023). For

structural health monitoring accelerometers on bridges or buildings, typical power budgets are 1-5 mW for continuous low-frequency vibration monitoring. Compared to the existing literature, our hybrid system's output power of 4.35 mW at 46.55 Hz demonstrates competitive performance in the context of compact energy harvesters. Toyabur et al. (Toyabur et al., 2018) achieved a maximum output power of 740 μW, with our system achieving nearly six times their total hybrid power output. A magnetically coupled piezoelectric-electromagnetic hybrid harvester (Junlei et al., 2020) reported 332 μW at a resonant frequency of 21.6 Hz, which is 13 times lower than our system's performance. Our 74% to 135% power improvement over single-transducer configurations validate the effectiveness of the parallel hybridization approach. The hybrid system is the most efficient solution compared to the single-transduction system, with optimization of the hybrid system highlighting the complementary nature of this vibrational energy recovery.

This study has significant limitations related to ideal simulation conditions that differ from reality, particularly actual vibrations (multifrequency and transient) that could reduce efficiency by 15 to 30%. Temperature variations (-20°C to +60°C) and manufacturing tolerances (±5% thickness, ±0.1 mm positioning) can affect material properties and introduce performance variability of 5 to 12%. Mechanical fatigue after millions of cycles can degrade the system, although PZT-5H retains 85 to 90% of its performance after 10^9 cycles. Environmental factors (humidity, shock, electromagnetic interference) require protective encapsulation, which was not modeled in this study. Despite these limitations, the 74 to 135% improvement of the hybrid system should persist under real-world conditions, but field testing is essential to quantify these effects and optimize the system.

6. Conclusion

This study demonstrates the superior performance of the hybrid system compared to single transducer systems for powering autonomous electronic devices. Simulations performed using COMSOL Multiphysics 6.2 confirmed a maximum power output of 4.35 mW at a resonant frequency of 46.5 Hz for the hybrid configuration. This represents a substantial improvement of 74% compared to the piezoelectric-only system (2.50 mW) and 135% compared to the electromagnetic-only system (1.85 mW). The parallel coupling of the two technologies allows their complementary advantages to be exploited: high voltage from the piezoelectric transducer and high current from the electromagnetic transducer. The hybrid system achieved a quality factor of 5.2, indicating excellent energy conversion efficiency at the resonant frequency. However, this comes with a trade-off: the system exhibits a reduced bandwidth of 9 Hz compared to individual transducers, making it particularly suitable for stable-frequency applications such as industrial machinery, HVAC systems, or vehicle engines where the operational frequency remains relatively constant. For applications with variable frequency vibration sources, this bandwidth limitation should be carefully considered. Despite this constraint, the 74% to 135% power improvement clearly demonstrates the effectiveness of the parallel hybridization approach. This optimized hybrid energy harvesting system ensures battery autonomy and avoids the use of electrochemical batteries for embedded systems and Internet of Things devices. The optimization of these hybrid microgenerators paves the way for increased energy autonomy in low-power electronic devices, offering a sustainable and maintenance-free power solution for wireless sensor nodes and IoT applications requiring 1–10 mW continuous power supply.

Declaration of Ethical Standards

As the authors of this study, we declare that it complies with all ethical standards. No human participants or animals were involved in this research.

Credit Authorship Contribution Statement

ATM: Conceptualization, Software, Formal analysis, Writing - Original Draft

RHA: Methodology, Validation, Visualization.

HEF: Supervision, Resources, Writing - Review & Editing, Project administration.

Declaration of Competing Interest

The authors declare that they have no known competing financial interests or personal relationships that could have appeared to influence the work reported in this paper.

Funding / Acknowledgements
I would like to express my sincere gratitude to Dr. Fils for his invaluable assistance and dedication throughout my research. My heartfelt thanks go to my family, whose encouragement pushed me to the finish line; they have been my greatest motivation.
As the authors of this study, we declare that generative AI was used only for language editing and not for scientific content generation.

Data Availability
The data that support the findings of this study are available within the article (see Tables 1, 2, and 3 for simulation parameters). No external datasets were generated or analyzed during the current study.

References

Ahmad M. & Khan F. (2020). Review of vibration-based electromagnetic-piezoelectric hybrid energy harvesters. International Journal of Energy Research, 45(4), DOI:10.1002/er.6253

Bing H., Shubin Z., Jianbin L., YanFeng J. (2022). Design and Development of a 2 × 2 Array Piezoelectric–Electromagnetic Hybrid Energy Harvester. Micromachines, 13(5), 752, https://doi.org/10.3390/mi13050752.

Cai M. & Liao W. H. (2020). Enhanced electromagnetic wrist-worn energy harvester using repulsive magnetic spring. Mechanical Systems and Signal Processing, 150(1):107251, DOI:10.1016/j.ymssp.2020.107251

Faraday, M. (1832). Experimental researches in electricity. Philosophical Transactions of the Royal Society of London, 122, 125–162. urn:doi:10.1098/rstl.1832.0006.

Han Yu, Xiaobiao S., Chengwei H., Xingxu Z. (2022). A novel seesaw-like piezoelectric energy harvester for low frequency vibration. SSRN Electronic Journal DOI:10.2139/ssrn.4134866.

Hao Y., Luo H., Lu X., Huang, J. (2024). Piezoelectric energy harvester with outstanding output performance at low frequency vibration based on concentrating force on the piezoelectric element by parallel springs. Journal of Applied Physics, 135(4), 045001, DOI:10.1063/5.0180931

Iqbal M., Nauman M. M., Farid K., Pg Emeroylariffion Abas (2020). Vibration-based piezoelectric, electromagnetic, and hybrid energy harvesters for microsystems applications: A contributed review. International Journal of Energy Research, 45(1), 1–38.

Jaspreet S. , Ranjit K., Damanpreet S. (2020). Energy harvesting in wireless sensor networks: A taxonomic survey. International Journal of Energy Research, https://doi.org/10.1002/er.5816

Jinhui Z., Maoyu L., Wei Z., Tao L., Lifeng Q. (2021). Modeling of a Rope-Driven Piezoelectric Vibration Energy Harvester for Low-Frequency and Wideband Energy Harvesting. Micromachines, 12(3), 305, https://doi.org/10.3390/mi12030305.

Joy A., Joshi V., Narendran K. & Ghoshal R. (2023). Piezoelectric energy extraction from a cylinder undergoing vortex-induced vibration using internal resonance. Scientific Reports, 13, 6924, DOI:10.1038/s41598-023-33760-5

Jung, I., Choi, J., Park, H. J., Lee, T. G., Nahm, S., Song, H. C., Kim, S., & Kang, C. Y. (2020). Design principles for coupled piezoelectric and electromagnetic hybrid energy harvesters for autonomous sensor systems. Nano Energy, 75, 104921, DOI 10.1016/j.nanoen.2020.104921

Junlei W., Linfeng G., Lin D., Hongjun Z. , Daniil Y. (2020). The state-of-the-art review on energy harvesting from flow-induced vibrations. Applied Energy, 267, 114902, https://doi.org/10.1016/j.apenergy.2020.114902

Liu H., Fu H., L., Sun L., Lee C. (2020). Hybrid energy harvesting technology: From materials, structural design, system integration to applications. Renewable and Sustainable Energy Reviews, 137:110473. DOI:10.1016/j.rser.2020.110473

Nejati S. A., Mostafa R. G., Farnoush N., Masoud N.T. (2024). A comprehensive review of energy harvesting and routing strategies for IoT sensors sustainability and communication technology. Sensors International, 5, 100258.

Toyabur R. M., Md Salauddin, Cho H.. & Park, J. Y. (2018). A multimodal hybrid energy harvester based on piezoelectric-electromagnetic mechanisms for low-frequency ambient vibrations. Energy Conversion and Management, https://doi.org/10.1016/J.ENCONMAN.2018.05.018.

Xutao M., Shengxi Z., Zhichun Y., Tsutomu K. (2021). Enhancing energy harvesting in low-frequency rotational motion by a quad-stable energy harvester with time-varying potential wells. Mechanical Systems and Signal Processing, 148:107167, DOI:10.1016/j.ymssp.2020.107167

Williams C., Christopher S., M.A. Harradine, P.H. Mellor (2002). Development of an electromagnetic micro-generator. IEE Proceedings - Circuits, Devices and Systems, 148(6), 337–342, DOI:10.1049/ip-cds:20010525

Zhongjie Li, Chuanfu X., Yan P., Min W. (2021). Power Density Improvement of Piezoelectric Energy Harvesters via a Novel Hybridization Scheme with Electromagnetic Transduction. Micromachines, 12(7):803, DOI:10.3390/mi12070803

Zhongjie Li, Yong Liu, Peilun Yin, Yan P. (2021). Constituting abrupt magnetic flux density change for power density improvement in electromagnetic energy harvesting. International Journal of Mechanical Sciences, 198, DOI:10.1016/j.ijmecsci.2021.106363.